

See discussions, stats, and author profiles for this publication at: <https://www.researchgate.net/publication/26835058>

Counterion Atmosphere and Hydration Patterns near a Nucleosome Core Particle

ARTICLE *in* JOURNAL OF THE AMERICAN CHEMICAL SOCIETY · SEPTEMBER 2009

Impact Factor: 12.11 · DOI: 10.1021/ja905376q · Source: PubMed

CITATIONS

32

READS

40

3 AUTHORS, INCLUDING:



[Garegin A Papoian](#)

University of Maryland, College Park

72 PUBLICATIONS 1,982 CITATIONS

SEE PROFILE

Counterion Atmosphere and Hydration Patterns near a
Nucleosome Core Particle

Christopher K. Materese, Alexey Savelyev, and Garegin A. Papoian*

Department of Chemistry, University of North Carolina at Chapel Hill, Chapel Hill, North
Carolina 27599-3290

Received June 30, 2009; E-mail: gpapoian@unc.edu

Abstract: The chromatin folding problem is an exciting and rich field for modern research. On the most basic level, chromatin fiber consists of a collection of protein–nucleic acid complexes, known as nucleosomes, joined together by segments of linker DNA. Understanding how the cell successfully compacts meters of highly charged DNA into a micrometer size nucleus while still enabling rapid access to the genetic code for transcriptional processes is a challenging goal. In this work we shed light on the way mobile ions condense around the nucleosome core particle, as revealed by an extensive all-atom molecular dynamics simulation. On a hundred nanosecond time scale, the nucleosome exhibited only small conformational fluctuations. We found that nucleosomal DNA is better neutralized by the combination of histone charges and mobile ions compared with free DNA. We provide a detailed physical explanation of this effect using ideas from electrostatics in continuous media. We also discovered that sodium condensation around the histone core is dominated by an experimentally characterized acidic patch, which is thought to play a significant role in chromatin compaction by binding with basic histone tails. Finally, we found that the nucleosome is extensively permeated by over a thousand water molecules, which in turn allows mobile ions to penetrate deeply into the complex. Overall, our work sheds light on the way ionic and hydration interactions within a nucleosome may affect internucleosomal interactions in higher order chromatin fibers.

1. Introduction

DNA in eukaryotic cells folds into a highly compact and hierarchically organized structure called chromatin.¹ Genomic DNA contains on the order of 10^9 base pairs, corresponding to a contour length on the scale of a meter, which must be compacted by many orders of magnitude to fit inside of a eukaryotic nucleus that is several micrometers in diameter. DNA is a highly charged macromolecule, carrying two negative elementary charges per base pair, making charge neutralization essential to diminish strong self-repulsion and allow the chain's compaction.² Additionally, DNA is a semiflexible polymer chain, with a persistence length of ~ 50 nm (at physiological conditions); thus, high level compaction would also incur elastic and entropic penalties.² These two problems are addressed to a significant extent through the formation of a DNA–protein complex, called a nucleosome (see Figure 1), in which the DNA associates with a protein histone core, the latter carrying a large net positive charge.³ Specifically, a nucleosome particle is composed of 146 DNA base pairs wrapped in ~ 1.7 turns around the core of the histone proteins. In addition to the histone core, neutralization of the remaining DNA charge is controlled by the surrounding aqueous salt environment. Aqueous salts play an important role in mediating various biological processes such as protein association,^{4,5} RNA folding,⁶ nucleosome formation⁷

and chromatin compaction. In this work we extensively study the environment of mobile counterions surrounding the nucleosome.

The nucleosome particle, together with the linker DNA segment connecting adjacent nucleosomes, represents a basic repeating unit of chromatin fiber.¹ The nucleosome complex may be viewed as the first, most basic level of the nuclear DNA compaction—subsequent compaction is achieved through the formation of secondary structure (30 nm fiber). The formation of the most basic chromatin structures are strongly dependent on the concentration of mobile ions in solution,⁸ whose role is to mitigate the electrostatic repulsion between linker DNA segments and also to mediate internucleosomal interactions. How mobile ions interact with both the nucleosomal DNA and the protein histone core is an important issue that has been largely overlooked in prior computational studies of nucleosome particles and polynucleosomal arrays.^{9–11} A precise description of site-specific electrostatics of the nucleosome is likely needed for an accurate description of chromatin folding. For example,

- (1) van Holde, K. E. *Chromatin*; Springer: New York: 1989.
- (2) Schiessel, H.; Gelbart, W. M.; Bruinsma, R. *Biophys. J.* **2001**, *80*, 1940–1956.
- (3) Luger, K.; Mder, A. W.; Richmond, R. K.; Sargent, D. F.; Richmond, T. J. *Nature* **1997**, *389*, 251–260.
- (4) Lund, M.; Jonsson, B. *Biophys. J.* **2003**, *85*, 2940–2947.

- (5) Chodankar, S.; Aswal, V. K. *Phys. Rev. E: Stat. Nonlin. Soft Matter Phys.* **2005**, *72*, 041931.
- (6) Koculi, E.; Hyeon, C.; Thirumalai, D.; Woodson, S. A. *J. Am. Chem. Soc.* **2007**, *129*, 2676–2682.
- (7) Schiessel, H. J. *Phys.: Condens. Matter* **2003**, *15*, R699–R774.
- (8) Bertin, A.; Mangenot, S.; Renouard, M.; Durand, D.; Livolant, F. *Biophys. J.* **2007**, *93*, 3652–3663.
- (9) Woodcock, C. L.; Grigoryev, S. A.; Horowitz, R. A.; Whitaker, N. *Proc. Natl. Acad. Sci. U.S.A.* **1993**, *90*, 9021–9025.
- (10) Langowski, J.; Heermann, D. W. *Semin. Cell Dev. Biol.* **2007**, *18*, 659–667.
- (11) Sun, J.; Zhang, Q.; Schlick, T. *Proc. Natl. Acad. Sci. U.S.A.* **2005**, *102*, 8180–8185.

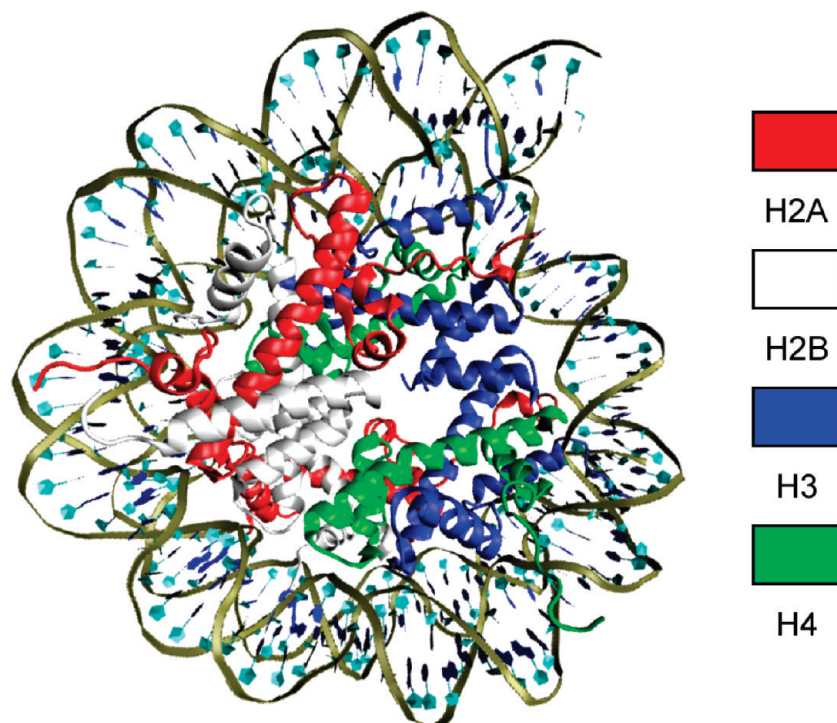


Figure 1. Yeast nucleosome used in this study (PDB entry 1id3) is shown here with its histone proteins color coded.

histone tails, which are flexible, highly charged, and unstructured portions of the main histone proteins, protrude from the nucleosome particle and mediate interactions between proximal nucleosomes.¹² Post-translational modifications of these tails, which alter their electrostatics, are among the primary mechanisms regulating chromatin folding.^{12,13} It was recently suggested that a specific localized acidic patch on the histone core may play an important role in chromatin folding by providing an interaction site for histone tails.^{3,14} Though histone tails are not considered explicitly in the present study, we will show that sodium ions act as a probe and condense strongly around this acidic patch.

Both histone tail modifications and alterations to the surrounding ionic solution result in substantial changes to the nucleosome's electrostatic environment and crucially affect the formation of higher-order chromatin structures. Thus, to tackle the larger problem of chromatin folding, greater knowledge is needed at an atomic scale about the complex electrostatics of linker DNA, the nucleosome core particle, and histone tails. In prior works, we have analyzed short-range electrostatics and the ionic atmosphere around linker DNA using all-atom molecular dynamics (MD) simulations.^{15–18} In subsequent work, we developed coarse-grained models for linker DNA and electrolyte solutions, derived systematically by matching molecular correlation functions with all-atom MD simulation

results.^{19,20} Analogously, it is expected that deeper understanding of the electrostatic environment of the nucleosome may be used to shed light on intermolecular forces driving chromatin folding.

In this work, we endeavor to provide new insights into the nature of the nucleosome complex in its native state by performing a computationally extensive, 200 ns, explicit-solvent MD simulation of the yeast nucleosome (*Saccharomyces cerevisiae*) immersed into physiological NaCl salt buffer. This simulation is an order of magnitude longer than a prior all-atom simulation of the nucleosome.²¹ The longer simulation is needed to ensure that sufficient time has expired for mobile ion equilibration.^{22,23} We study the extent of the charge neutralization of the DNA surrounding the nucleosome. For added detail, we compute one- and two-dimensional radial distribution functions (RDFs), to identify spatially inhomogeneous association of mobile ions with DNA and histone proteins. Finally, we examine the high solvent accessibility of the nucleosome complex by identifying and visualizing water molecules residing inside the protein histone core and in between nucleosomal DNA strands.

The main results of the present study are as follows: It has been suggested that the complexation of the nucleosome core particle is driven in a part by the entropy gain from counterion release.⁷ In this work, we find that positive histone charges displace mobile counterions at a ratio that is larger than expected from simple counterion condensation arguments. We provide a detailed analysis of the causes of the excess positive charge and show that it is a result of multiple factors: First, the close

(12) Fischle, W.; Wang, Y.; Allis, C. D. *Curr. Opin. Cell Biol.* **2003**, *15*, 172–183.

(13) Strahl, B. D.; Allis, C. D. *Nature* **2000**, *403*, 41–45.

(14) Zhou, J.; Fan, J. Y.; Rangasamy, D.; Tremethick, D. J. *Nat. Struct. Mol. Biol.* **2007**, *14*, 1070–1076.

(15) Savelyev, A.; Papoian, G. A. *J. Am. Chem. Soc.* **2006**, *128*, 14506–14518.

(16) Savelyev, A.; Papoian, G. A. *Mendeleev Commun.* **2007**, *17*, 97–99.

(17) Savelyev, A.; Papoian, G. A. *J. Am. Chem. Soc.* **2007**, *129*, 6060–6061.

(18) Savelyev, A.; Papoian, G. A. *J. Phys. Chem. B* **2008**, *112*, 9135–9145.

(19) Savelyev, A.; Papoian, G. A. *Biophys. J.* **2009**, *96*, 4044–4052.

(20) Savelyev, A.; Papoian, G. A. *J. Phys. Chem. B* **2009**, *113*, 7785–7793.

(21) Roccato, D.; Barthel, A.; Zacharias, M. *Biopolymers* **2007**, *85*, 407–421.

(22) Ponomarev, S. Y.; Thayer, K. M.; Beveridge, D. L. *Proc. Natl. Acad. Sci. U.S.A.* **2004**, *101*, 14771–14775.

(23) Varnai, P.; Zakrzewska, K. *Nucleic Acids Res.* **2004**, *32*, 4269–4280.

wrapping of DNA leads to an additive effect of the electric fields produced by the DNA and causes an increase in sodium condensation relative to that normally observed in free DNA. Second, the difference in dielectric constants between the water and the histone core that the DNA encircles creates a mirroring effect that enhances sodium condensation. Third and finally, immobilizing some counter charges near the DNA leads to an overall enhancement of the charge neutralization. As a corollary to our findings, the histone core, in conjunction with counterions, is better able to neutralize the charge of the encircling DNA than what monovalent counterions alone accomplish on free, unbound segments of DNA, likely resulting in reduced internucleosomal repulsion in compact chromatin fibers. Furthermore, this may also explain the experimentally observed preference for positively charged histone tails to bind to linker DNA as opposed to nucleosomal DNA.^{24,25}

In addition to the expected high density of sodium condensation on the nucleosomal DNA, we also revealed highly localized sodium condensation on the largely positively charged histone core around sites consisting of predominately acidic residues. The most significant sodium condensation occurs at the acidic patch, which is suggested to play a significant role as a potential internucleosomal interaction site for histone tail binding.^{3,14} We suggest that this finding adds new insight to the theory regarding histone tail binding to the acidic patch in that in addition to the assumed electrostatic favorability of association, there is also an entropic gain due to the release of counterions from the site.

We also found over a thousand water molecules extensively permeating the nucleosome particle interior, likely increasing the average interior dielectric constant from around 2–4, commonly used to model proteins. Thus, as a physical object, nucleosome core particle resembles a sponge. This, in turn, allows mobile ions to easily penetrate the complex interior.

In summary, our extensive all-atom simulation provides new insight and understanding of the nucleosome core particle.

2. Methods

2.1. Simulation Details. An all-atom molecular dynamics simulation of a yeast nucleosome was performed using the CHARMM27 protein–nucleic acid force field²⁶ and the NAMD program suite.²⁷ A yeast nucleosome, (*Saccharomyces cerevisiae*), PDB entry 1ID3, was taken as the initial structure²⁸ (Figure 1). Aspartic and glutamic acid residues were assigned to be negatively charged, while lysines and arginines were assigned to be positively charged. The 17 histidine residues in the histone core were assigned to their neutral state with a single proton at the N^{ε2} position; however, this residue may be protonated in the N^{δ1} site or doubly protonated, where the latter is expected at slightly acidic pH. The simulation was performed with over 54 000 explicit TIP3P water molecules in a box with the dimensions $\approx 135 \times 109 \times 140 \text{ \AA}^3$. The simulation was performed under periodic boundary conditions with a minimum of 30 Å between nucleosomes in neighboring cells. The total system charge was neutralized by the addition of sodium counterions, followed by the subsequent introduction of an additional 150 mM NaCl to approximate physiological conditions. The system was initially held at constant volume, and the

nucleosome was frozen in place while the water and ions were minimized for 100 000 steps. Subsequently, all constraints were removed from the system and it was minimized for an additional 400 000 steps. The system was gradually heated from 0 K via Langevin dynamics to 300 K in incremental steps of 5 K every 10 ps.

The production run proceeded with 2 fs time steps using the SHAKE algorithm and Ewald summation for long-range interactions. Weak harmonic positional restraints of $5 \times 10^{-5} \text{ kcal/mol \AA}^2$ were used to prevent large-scale translation or rotation of the nucleosome in an asymmetric box, however, small- and medium-scale nucleosomal motions were not affected. Short-range non-bonded interactions were calculated at each step, long-range interactions were calculated on even steps only, and the pair list was updated every 10 steps. System coordinates were saved every 1000 steps (2 ps) for later analysis. The production run was conducted under the constant pressure, moderated by Langevin piston (set to 1 atm), with a total simulation time of 200 ns ($\sim 205\,000$ CPU hours using 2.3 GHz Intel EM64T processors).

2.2. Verification of Convergence. It was shown previously that 50 ns was needed to equilibrate ions near DNA chains.^{22,23} To verify the validity of this assumption in our simulation, we divided the trajectory into four 50 ns sections and computed radial distribution functions for each section individually. The only significant change was observed between the first 50 ns and the rest of the trajectory. During the first 50 ns, the first two peaks of the nucleosome-sodium RDF showed a subtle shift of some sodium from the second peak to the first. We did not observe any significant changes in nucleosome-ion RDFs after the first 50 ns. The total number of ions within 1 nm of DNA was stable throughout the entire 200 ns of the simulation (191 ± 0.9). As an additional check, we tracked ions in the histone core and found that the vast majority of ion condensation events (approach of within 7 Å of nucleosome) were vanishingly short with only 1.7% of condensations lasting for more than 1 ns and only 0.1% of condensations lasting for more than 10 ns. We observed a single long-lived condensation event that lasted for more than 100 ns, which is elaborated upon below. These collective results suggest that though there may be a few highly specific sites that have not reached equilibration, the number of these sites is exceedingly small and has little effect on the primary conclusions of this work.

2.3. Analysis of Counterions with All-Atom MD. A standard method for analyzing counterion distribution in solution is to compute a radial distribution function (RDF). The first step in the creation of a nucleosome-counterion RDF involves computing the distance between each ion in the system and the nearest atom in the nucleosome at each time step. These data are then histogrammed and normalized by a volume Jacobian to obtain the RDF. The Jacobian was obtained numerically and was defined for each distance as the total volume of a discrete shell defined in a 3-D cubic lattice at that distance from the nucleosome. The bin size for the RDF histogram and the lattice apportionment size for the Jacobian calculation were both 0.5 Å. Because the nucleosome is a highly rigid molecule, the Jacobian was only recomputed every 1000 time steps. All in-house analysis programs were written with the assistance of the Biochemical Algorithms Library (BALL).²⁹

We have also visualized ion density in 3-D through use of a technique that can be paralleled to long exposure photography. First, overall translation and rotation of the nucleosome are removed from the trajectory through least-squares fitting to the crystal structure. Then, simulation box is divided into $1.5 \times 1.5 \times 1.5 \text{ \AA}^3$ cells and the location of each ion is recorded for the entire length of the simulation. Each cell is then assigned an average ion concentration.

2.4. Analysis of Counterions with the Poisson–Boltzmann Equation. In addition to our all-atom studies, we have performed mean-field electrostatics calculations using the Poisson–Boltzmann formalism. For this work we used the Adaptive Poisson–Boltzmann Solver (APBS)³⁰ program suite. A $257 \times 193 \times 257$ rectangular

(24) Pruss, D.; Wolffe, A. P. *Biochemistry* **1993**, *32*, 6810–6814.

(25) Angelov, D.; Vitolo, J. M.; Mutskov, V.; Dimitrov, S.; Hayes, J. J. *Proc. Natl. Acad. Sci. U.S.A.* **2001**, *98*, 6599–6604.

(26) MacKerell, A. D.; Banavali, N.; Foloppe, N. *Biopolymers* **2000**, *56*, 257–265.

(27) Phillips, J. C.; Braun, R.; Wang, W.; Gumbart, J.; Tajkhorshid, E.; Villa, E.; Chipot, C.; Skeel, R. D.; Kal, L.; Schulten, K. *J. Comput. Chem.* **2005**, *26*, 1781–1802.

(28) White, C. L.; Suto, R. K.; Luger, K. *EMBO J.* **2001**, *20*, 5207–5218.

(29) Kohlbacher, O.; Lenhof, H. P. *Bioinformatics* **2000**, *16*, 815–824.

Table 1. Summary of Results from Our All-Atom Nucleosome Simulation Describing the Charge Distribution within 1 nm of the DNA Surface

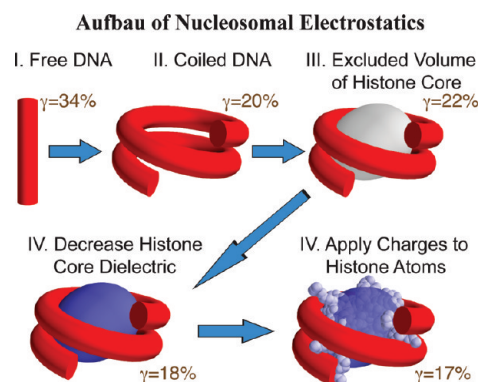
	charge	% of DNA charge
Net charge of DNA	−292	100%
Net charge of counterions	174	60%
Net charge of histones	76	26%
Net charge of system	−42	$\gamma = 14\%$
Radial center of mobile charges	4.40 Å	
Radial center of protein charges	4.34 Å	

grid with a step size of 0.78 Å was used for the P–B calculation. Sodium and chloride bulk concentrations were both set to 150 mM and the solvent probe radius was set to 1.4 Å. Solute and solvent dielectrics were set to 3.0 and 78 respectively. APBS was used to solve the nonlinear P–B equation with the boundary condition potential specified by a Debye–Hückel model for multiple, noninteracting spheres. Identical parameters were used in calculations of one and two DNA chain systems, however, in these cases the grid step size was roughly halved (varying slightly between systems). Computation of RDFs arising from P–B results was carried out using similar methods to those previously used for all-atom results.

3. Results and Discussion

3.1. Nucleosome is Highly Rigid on a 200 ns Time Scale. The first goal of our study was to characterize the conformational dynamics of the nucleosome on a 200 ns time scale. Visually, the structures appear remarkably similar throughout the simulation, except for a minor difference in the orientation of the loose entry and exit ends of the DNA, which are not tightly bound to histone core and are exposed to the solvent. To quantitatively examine this issue, we used dihedral angle principal component analysis to characterize the nucleosome's dynamics, similar to earlier work.³¹ This technique revealed the presence of several dynamical basins in the space described by the first two principal components (data not shown). However, representative structures from the most dissimilar basins were found to be within ~ 3 Å rmsd from each other. The robustness of the nucleosomal structure is subsequently useful later in this article when we generate a 3-D time averaged ion and water density plots around the nucleosome. In summary, on a 200 ns time scale, the nucleosome appears to undergo only small-scale structural fluctuations.

3.2. Nucleosomal DNA is More Neutralized than Free DNA. The primary goal of our study was to characterize the counterionic environment surrounding the nucleosome. For this discussion, we introduce the quantity γ , which is the percentage of the residual DNA charge after accounting for counterions and histone charges within 1 nm of the DNA surface. As a first step, we computed γ from our all-atom simulation. The results of this calculation are shown in Table 1. Previous work has suggested that mobile ions are able to neutralize $\sim 75\%$ ($\gamma = 25\%$) of the charge of a strand of free DNA at a distance of 0.9–1 nm.^{15,32–34} The DNA surrounding the nucleosome has a charge of −292, therefore we would expect ~ 219 of these charges to be neutralized by counterions. The histone core

**Figure 2.** Conceptual step by step nucleosomal assembly pathway for understanding the effects of nucleosome formation on counterion condensation.

provides a net charge of +76 within 1 nm of the DNA; therefore, a release of 76 mobile counterions is anticipated if we assume a 1 to 1 replacement. However, we observed a net +174 charge from counterions within 1 nm, indicating that only 45 counterions were released, instead of expected 76. This means that the histone and counterions collectively reduce residual DNA charge from $\gamma = 25\%$ in free DNA to $\gamma = 14\%$. Since this phenomenon results from multiple effects, we attempt to provide a clear explanation through a hypothetical, step-by-step, nucleosome assembly process (Figure 2). For each step, we performed an extensive series of nonlinear Poisson–Boltzmann calculations to demonstrate how that particular step alters counterionic atmosphere around DNA.

Our assembly process starts (**State I**) with a strand of free DNA in a mean field solvent and salt bath (150 mMol NaCl). In this state, we computed $\gamma = 34\%$ for the residual charge of DNA at 1 nm. It should be noted that this result is a higher baseline than predicted by Manning³⁴ and our previous all-atom simulations.¹⁵

Next, as an approximation of the real system, we measured the effect of bringing together two parallel strands of DNA from an initially large distance, to mimic the effect of **State II**. As shown in Figure 3a, counterion condensation monotonically increases as the DNA center to center chain distance decreases as an effect of the combination of the electric fields created by each strand. Bringing two DNA strands from an infinite separation to within a few Angstroms of one another has a similar effect to increasing the charge density on a single strand, which is expected to result in enhanced condensation to lower the line charge density down to the Manning threshold. At the inter-DNA separation found in the nucleosome, this effect brings the DNA residual charge from $\gamma = 34\%$ to $\gamma = 23\%$. We observed similar, but less pronounced, results from prior all-atom simulations,¹⁷ where we measured a $\gamma = 26\%$ to $\gamma = 18\%$ change in DNA residual charge. If instead of two parallel strands of DNA we perform a PB calculation with the coiled DNA from the nucleosome PDB with the histone cores removed, we observe a small change from $\gamma = 23\%$ to $\gamma = 20\%$. This is likely a result of the curved geometry of the DNA chain in the latter as opposed to the two linear strands used in the former case.

The next step of inserting a histone core into spiral-shaped DNA chain introduces multiple effects due to: (1) excluded volume, (2) low dielectric, and (3) immobilized histone charges. These effects change the extent of counterionic condensation in profoundly different ways. Thus, to individually understand each of these effects, we subdivided the histone insertion into

(30) Baker, N. A.; Sept, D.; Joseph, S.; Holst, M. J.; McCammon, J. A. *Proc. Natl. Acad. Sci. U.S.A.* **2001**, *98*, 10037–10041.

(31) Materese, C. K.; Goldmon, C. C.; Papoian, G. A. *Proc. Natl. Acad. Sci. U.S.A.* **2008**, *105*, 10659–10664.

(32) Manning, G. S. *J. Chem. Phys.* **1969**, *51*, 924–933.

(33) Feig, M.; Pettitt, B. M. *Biophys. J.* **1999**, *77*, 1769–1781.

(34) Manning, G. S. *J. Am. Chem. Soc.* **2003**, *125*, 15087–15092.

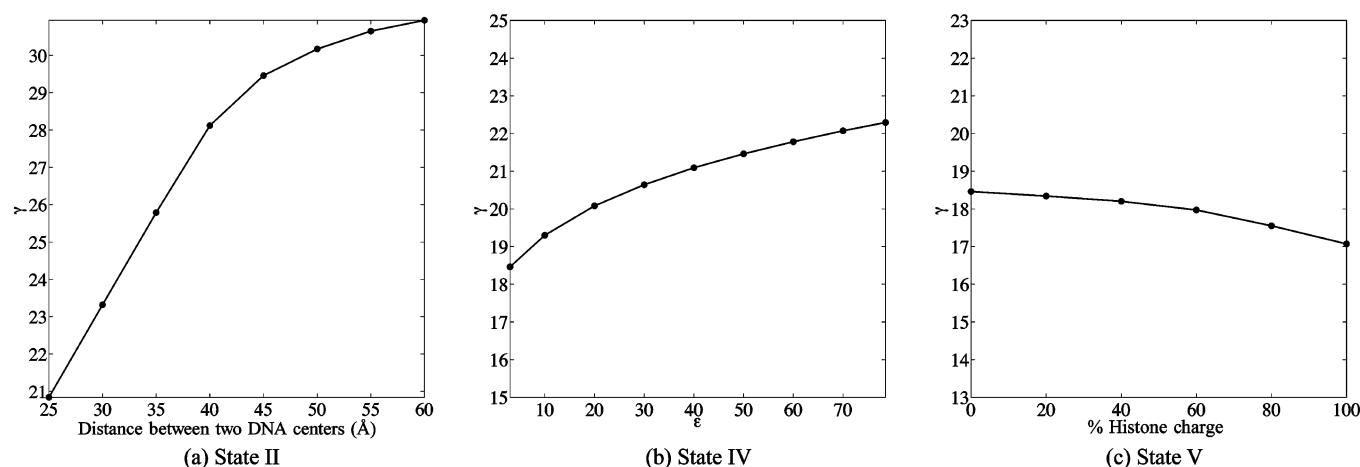


Figure 3. Percent of DNA charge neutralization (a) of two strands of parallel DNA at multiple distances between the centers of the DNA strands, (b) of the nucleosomal DNA wrapped around a histone core with different dielectric constants, and (c) of the nucleosomal DNA with the charges of the histone core uniformly scaled.

several substeps. In **State III**, to reveal the effect of the excluded volume interactions, we introduce a completely neutral histone core, impermeable to the ionic bath, and with the same dielectric constant as the outside solvent. The effect of this excluded volume is a small change in residual DNA charge from $\gamma = 20\%$ to $\gamma = 22\%$.

In **State IV**, we continue to keep the histone core devoid of any charge, however, we reduce the dielectric constant of the material from that of the solvent $\epsilon \approx 78.54$ to $\epsilon \approx 3.0$ (however, this might significantly underestimate the dielectric constant of nucleosome complex if treated as a continuum material, as discussed below). It has been argued that the assignment of a dielectric constant for a protein in a PB system is nontrivial, and a higher value may be more appropriate.³⁵ Thus, the results from this section may be scaled but the trends should be the same. The effect of the reduction of the core dielectric (Figure 3b) can be explained by the dielectric mirroring effect in which the higher permittivity of the solvent keeps the force lines resulting from DNA electric field in the solvent, effectively creating an image charge of the same sign within the lower dielectric material.³⁶ As the dielectric constant of the histone core is decreased, counterion condensation increases, since the image charge effect grows stronger. This leads to a change in residual DNA charge from $\gamma = 22\%$ to $\gamma = 18\%$.

Finally, in **State V**, we gradually introduce the histone charges (Figure 3c) by uniformly changing the normal atom charges with a constant scaling factor and observe a final small change in residual DNA charge from $\gamma = 18\%$ to $\gamma = 17\%$. Using the analytical solution of the Poisson–Boltzmann equation for a solution of uniformly charged cylinders,³⁷ we found qualitatively similar results. Although in the case of the nucleosome this effect is small, it can become quite significant, when around 50% of mobile charges become stationary. To explain this effect we consider that the introduction of immobile positive charges from the histone core effectively reduces the DNA line charge density. Despite the fact that such a system results in diminished counterion condensation, we still find a net increase in DNA neutralization

when we retroactively subtract the immobilized charges from the DNA line charge and add them to the total number of counterions. Since the counterion condensation profile results from competition between electrostatics and mobile ion translational entropy, making some mobile ions stationary reduces the entropic penalty, allowing larger overall charge neutralization.

Poisson–Boltzmann results indicate that the most significant contribution to DNA charge neutralization is simply the result of the enhancement of the electric field caused by the tight wrapping of the DNA chain around the histone core. However since Poisson–Boltzmann results are not entirely numerically consistent with all-atom observations it is possible that the relative importance may shift between these effects. Further numerical experiments based on all-atom simulations could be used to examine the magnitude of each effect.

To verify that the electrostatic interactions between DNA and positively charged histone residues were not significantly diminished because of the latter being deeply buried, we defined an effective radial center of the charge distribution within 1 nm of the DNA for both the charged histone residues and the ions in solution using the same method as would be used to compute a center of mass. We find that both the histone core and the mobile ions possess nearly the same center of charge (Table 1). This means that within 1 nm, the average distance of a charged residue to the DNA chain is the same as the average distance of an ion to the DNA chain. There are 13 histidine residues within 1 nm of DNA that could become protonated under slightly acidic conditions. Protonation of these sites could cause some additional counterion release, increasing nucleosomal stability, but we do not expect this change to significantly alter our conclusions. Collectively, these results likely carry significant consequences for higher order chromatin compaction, because they demonstrate that the combination of a histone core and monovalent counterions is more effective at neutralizing the charge of a segment of DNA up to a distance of 1 nm than if the same segment were in the presence of only the counterions. It has been noted that some histone tails preferentially bind to linker DNA over nucleosomal DNA.^{24,25} We postulate that this effect may in part be caused by the increased charge neutralization of nucleosomal DNA relative to linker DNA.

3.3. High-Resolution Description of Counterionic Atmosphere.

As a next step, we computed nucleosome-sodium RDFs for both all-atom and mean-field Poisson–Boltzmann results (Figure 4). Both results showed a significant increase in sodium concentra-

(35) Warshel, A.; Sharma, P. K.; Kato, M.; Parson, W. W. *Biochim. Biophys. Acta* **2006**, 1764, 1647–1676.

(36) Dobrynin, A. V.; Rubinstein, M. *Prog. Polym. Sci.* **2005**, 30, 1049–1118.

(37) Deshkovski, A.; Obukhov, S.; Rubinstein, M. *Phys. Rev. Lett.* **2001**, 86, 2341–2344.

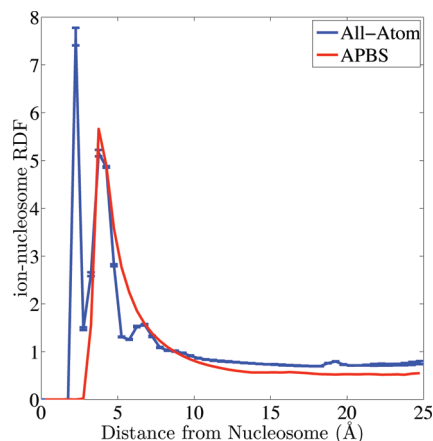


Figure 4. Comparison of the 1-D sodium-nucleosome radial distribution functions obtained from APBS and all-atom simulations reveals important qualitative difference. Specifically, the first peak of the all-atom result, indicative of sodium condensation is absent from the mean field result. The all-atom plot is averaged from the final three 50 ns segments with error bars shown for each point.

tion around the nucleosome relative to that of the bulk, which is unsurprising given the large net negative charge of the DNA histone complex. Significant qualitative differences, however, exist between the all-atom and the mean-field results. Three distinct ionic shells surrounding the nucleosome were observed in atomistic simulations, while the PB calculations lack this fine detail and show one single peak. This is anticipated because P-B calculations neglect the discrete nature of water and ions. A similar result was found in our previous work where ion condensation around a segment of linker DNA was analyzed using atomistic and mean field calculations.¹⁵ As discussed in our previous work, the single P-B peak near the nucleosome is equivalent to the second peak from the all-atom result while the first peak is absent. This first peak is representative of direct association of ions with the nucleosomal atoms. As with linker DNA, the strong close condensation of ions around the nucleosome significantly reduces the short-range (<1 nm) nucleosomal charge and may promote folding of a polynucleosomal array into chromatin fiber.

While a nucleosome-sodium RDF can provide useful information about the surrounding ionic environment, its resolution is very low. The nucleosome is far from a homogeneous object and is large relative to the length scale of interesting ionic condensation. As previously stated, the histone core has a large net positive charge, while the surrounding DNA is highly negatively charged. The dissimilarity between the two components of this system suggests that there is likely a significant difference between the propensity for a sodium ion to associate with DNA compared with histones. To address this issue, we have computed two-dimensional RDFs. The first dimension was chosen to be the distance between a sodium ion and the closest atom belonging to the DNA chain, while the second dimension corresponds to the distance between that same sodium atom and the closest atom belonging to the protein core. Two dimensional RDFs were created for the all-atom systems (P-B results are qualitatively similar with the same deviations observed in the 1-D case) with interesting results (Figure 5). Unsurprisingly, sodium ions preferentially associate with DNA; however, we also observed a significant condensation of sodium around the histone protein at locations distant from the DNA.

To understand the source of the sodium concentration around the histone core, we scanned the all-atom trajectory, selectively

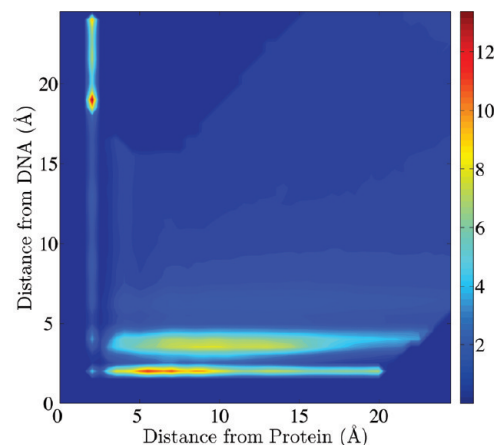


Figure 5. Two-dimensional sodium-nucleosome radial distribution function obtained from our all-atom simulation shows the layering of the sodium cloud around the DNA as shown in our 1-D result. It also reveals strong, highly localized sodium condensation on the histone core.

choosing only the ions within the two-dimensional RDF region identified by our plots. These sodium atoms were then examined against all residues of the nucleosome to identify the closest. It was found that this peak did not correspond to a large condensation at a single location, but contributions arose from several locations around specific residue types. Dense sodium condensation was observed primarily in regions rich in solvent accessible acidic residues. The plurality of the sodium condensation, 46%, was found closest to glutamic acid residues (negatively charged), followed by aspartic acid (negatively charged), 19%, and serine (neutral; polar), 19%. To further explore this issue, we also extended the search to include neighboring residues on the nucleosome. The results showed that ions condense most significantly when there are two or more acidic residues in close proximity.

Curiously, we identified a single condensation site around which the surrounding residues within ~ 7 Å (the Bjerrum length in water) possessed no excess of negative charge. We found that this condensation could be attributed to a single sodium atom in the interior of the histone core that occupied the site for over 100 ns and had not left by the end of the simulation. Visual inspection of the sight revealed that the sodium was forming a chelate complex with carboxylate group on the aspartic acid, a carbonyl oxygen on the serine backbone, and the hydroxyl group on the serine side chain (Figure 6). Thus, we hypothesize that the highly localized favorable interaction with these chelating oxygens and the associated entropy gain by sodium's ionic shell waters released into the bulk provided the remarkable longevity of the occupancy. While it is possible that there exist other neutral sites capable of chelating a sodium ion, we do not believe that this effect would be of much significance in terms of internucleosomal interactions because of steric considerations.

We compared our detailed sodium condensation data with a crystallographically identified acidic patch,³ which may play a significant role in internucleosomal interactions, and discovered that this patch was responsible for much of the observed sodium condensation. This observation may provide an additional suggestion regarding the method of histone tail association. In addition to the expected electrostatic favorability of bringing the basic residues of the histone tail in contact with the acidic patch, we now also expect there to be an entropic gain associated with counterion release from the site upon binding. Additionally,

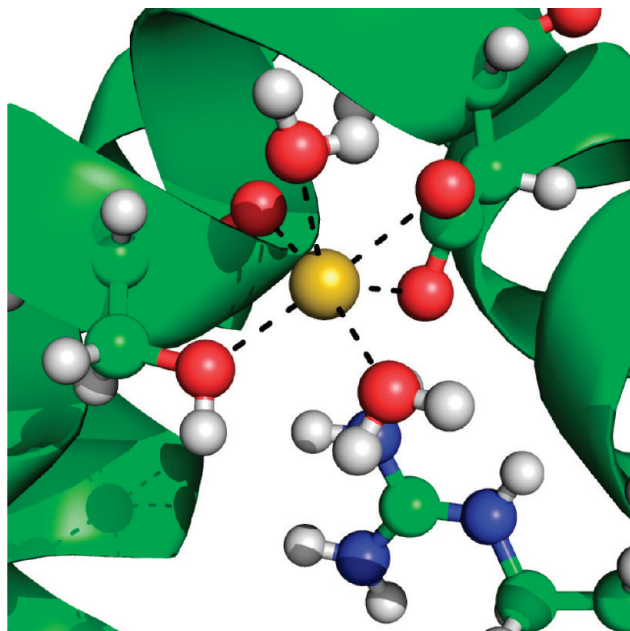


Figure 6. Long-lived chelate complex formed between a sodium ion (yellow) and oxygens (red) from the carboxylate group of a nearby aspartic acid residue in addition to both the backbone carbonyl and side chain hydroxyl group on a nearby serine residue (the atoms of the amino acid triplet and water in the first solvation shell around the sodium is shown as spheres).

this is exciting because it may be possible to use counterion condensation data to search for other potential internucleosomal

interaction sites *in silico*. In addition to radial distribution functions, we also produced a 3-D mapping of sodium density around the nucleosome (Figure 7). This plot clearly identifies the high level of sodium condensation around both the DNA and around the crystallographically identified acidic patch.

3.4. Nucleosome as a Sponge Filled with Water. Examination of the 3-D sodium density revealed ion penetration into the interior of the histone core, such as the previously described case of the chelated sodium. We verified that these ions were not present at the start of the simulation, naturally leading to the conclusion that they had arrived at some later time. This unanticipated result led us to examine the permeability of the histone core to the solvent. Crystallographic experiments have shown the presence of solvent within the core and the existence of significant water mediated interactions.³⁸ In a similar fashion to our sodium density calculations, we computed a 3-D solvent density of a space that can be described as an imaginary capsule capable of encompassing the interior of the histone core (Figure 8). Our analysis revealed an enormous solvent accessibility of the interior of the histone core. Although individual histone monomers effectively exclude water from their positions within the core, the space between histones is significantly solvated with a very large solvent channel in the center perpendicular to the DNA wrapping. This yields two important observations: First, the solvent allows ions to penetrate the core and may provide a local stabilization in regions of numerous like charges. Second, the solvent permeability mitigates the effect of the large net charge of the histone core by effectively providing a high dielectric bath. This emphasizes the need for a more detailed description of the core in the context of chromatin folding, which

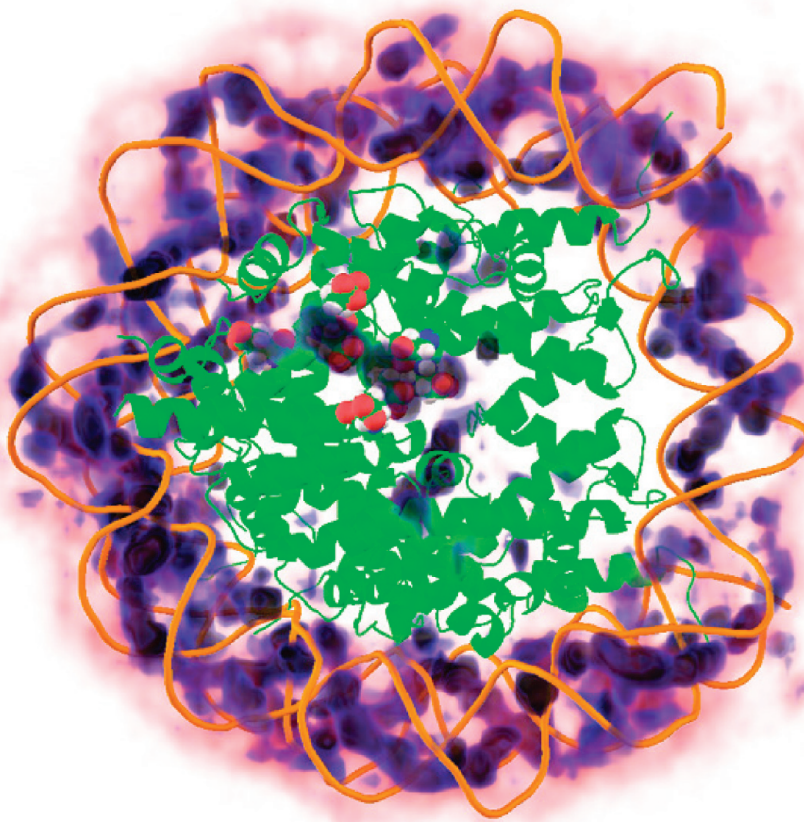


Figure 7. Three-dimensional distribution of sodium around the nucleosome. The crystallographically identified acidic patch has been highlighted as spheres on the surface of the histone core and a high level of sodium condensation is observed around these residues.

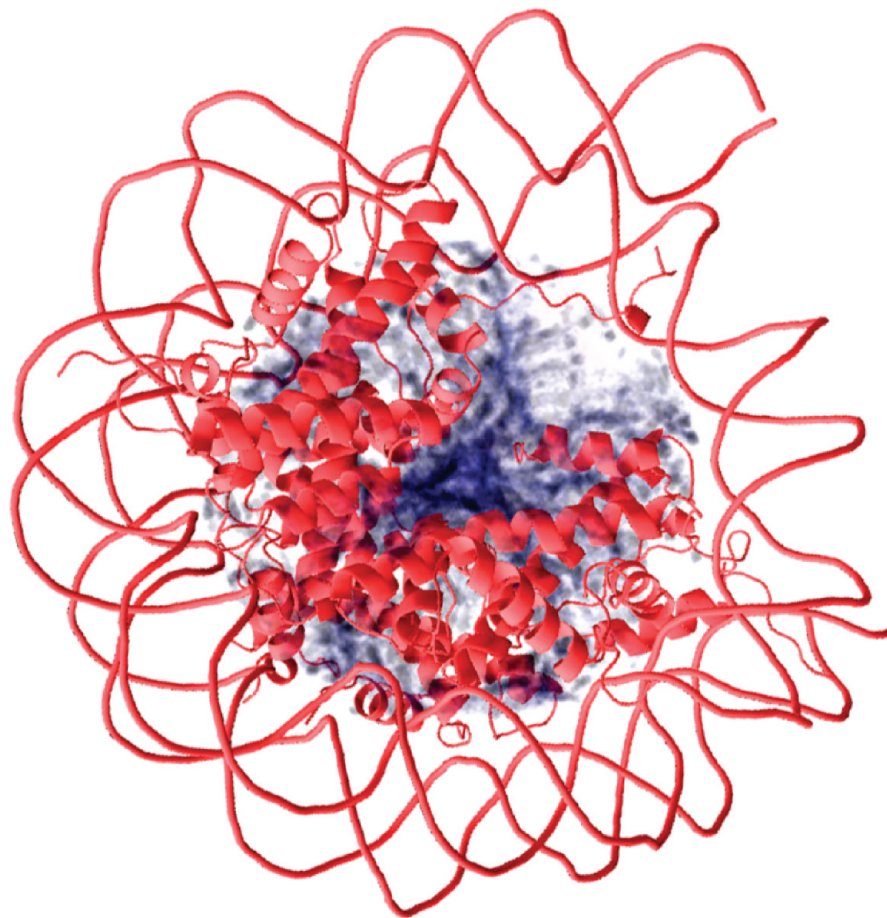


Figure 8. The core of the nucleosome is highly solvated as shown in this volumetric plot of water density. One H2 histone has been removed for clarity.

is almost always overlooked in modern coarse grained models of chromatin.

We also investigated the solvent mobility in the core to understand whether or not the water was more significantly structured in the core than in the surrounding solvent. We first computed a radial distribution function between the nucleosome and the oxygen atom of surrounding water molecules and determined the depth of the first solvation layer. From there, we computed autocorrelation functions of the water dipole moments within the first solvation layer and compared them with bulk water outside of this layer in the cases of both the interior and exterior of the nucleosome. Unsurprisingly, external bulk water was highly mobile with the average autocorrelation decaying to less than 10% after 10 ps. This result stands in stark contrast to water within the first hydration layer on the exterior of the nucleosome. These waters were highly structured and retained an average autocorrelation of ~65% after 10 ps, only decaying to ~40% after 100 ps (the size of our autocorrelation windows). Though autocorrelation of the dipole bond vectors can not produce meaningful rotational diffusion constants,³⁹ they still provide a useful gauge of the relative mobility of the selected water. We found no significant changes in these autocorrelation functions between interior surface waters and exterior surface water. Additionally, there was also no significant

change between the small amount of interior bulk water and exterior bulk water. Our results suggest that the majority of the water (~950 molecules) in the interior of the nucleosome are significantly constrained in dynamics, to the same extent as exterior water that resides within the first hydration layer. However, there is a significant amount of water (~200 molecules) in the core that behaves in a bulk-like fashion.

4. Conclusions

In this work, we described the ionic atmosphere around the nucleosome complex with atomic detail from an extensive, 200 ns all-atom MD simulation of the yeast nucleosome. We analyzed conformational rearrangements over the course of the MD simulation using dPCA and concluded that although the nucleosome is dynamic, large scale conformational changes are minimal over the accessible time scale.

Because subtle electrostatic effects play a crucial role in the process of condensation and decondensation of chromatin fiber, the need to understand electrostatics on the level of a single nucleosome particle arises naturally. We found in this work that the combination of the histone core and mobile counterions is more effective at neutralizing the DNA charge on a short, 1 nm length scale than mobile counterions alone. We demonstrated that this effect is a combination of 4 factors: First, winding the DNA around the histone core results in an additive combination of the electric field between closely wrapped bases and an increase in sodium condensation and thus greater charge

(38) Davey, C. A.; Sargent, D. F.; Luger, K.; Maeder, A. W.; Richmond, T. J. *J. Mol. Biol.* **2002**, *319*, 1097–1113.

(39) Zhang, Z.; Berkowitz, M. L. *J. Phys. Chem. B* **2009**, *113*, 7676–7680.

neutralization. Second, the excluded volume consumed by the histone core causes a slight reduction in the ability of mobile counterions to neutralize the DNA chain. Third, the differences between the solvent and histone core dielectric constants creates image charges of the DNA charge that increases sodium condensation and charge neutralization. Finally, the stationary positive histone charges also cause an increase in charge neutralization. Our results emphasize the role of proximal DNA chain interactions within a single nucleosome: wrapping DNA around the histone core results not only in significant elastic penalty but also in unfavorable inter-DNA electrostatic repulsion, where the latter effect is mitigated by additional counterion condensation. Thus, these unfavorable interactions must be overcome by both the free energy gain due to released counterions upon histone core insertion, and a combination of hydrophobic and hydrogen bond interactions between the histone core and the DNA. Larger neutralization of DNA in a nucleosome is expected to diminish internucleosomal repulsion in higher order chromatin arrays and may play a role in determining preferential binding of histone tails to linker DNA.

To obtain a more detailed description of the ionic atmosphere around the nucleosome, we computed one- and two-dimensional distribution functions of the surrounding ions. The results indicate that sodium ions condense primarily on the DNA molecule, as expected from simple electrostatic arguments, exhibiting characteristic patterns of pronounced peaks and minima in the 1D ion-DNA RDF, due to hydration shells. Far less trivial behavior was observed for the ions interacting with the protein part of the nucleosome, far from the DNA. Specifically, sodium seemed to heterogeneously condense around a localized region of acidic residues, which are required for nucleosome array folding.¹⁴ Hence, we suggest that in addition to the electrostatic favorability of binding between the

acidic patch and the basic residues of the histone tail, there may also be a favorable entropic effect created by the release of counterions from the patch site upon binding.

In this work, we found that the interior of the nucleosome core particle is highly solvent accessible and contains both surface and bulk-like water. This conclusion is consistent with the recently resolved crystal structure of the nucleosome core particle demonstrating the presence of many water molecules mediating histone-DNA interactions and the interaction among various core histone proteins.³⁸ However, this result runs contrary to many simplified models that treat the nucleosome as a dense, water impermeable, homogeneous, solid-like object with low dielectric constant. The results of the present study indicate that in simplified, coarse-grained representation of the nucleosome, the effect of solvent will have to be taken into account by setting a significantly higher dielectric constant, than is customarily used ($\epsilon \approx 2-4$). Finally, solvent accessibility appears to be responsible for the penetration of ions deep into the core of nucleosome. Particularly, we observed a remarkably long-lived sodium condensation in the protein histone core, where the ions may form a chelate complex with the residues of histone protein.

In summary, our work provides a detailed atomistic picture of the nucleosome complex in its native state. New insights into the nucleosome core particle ionic atmosphere, solvent accessibility and dynamics point to important details that may help to better understand and model structure and dynamics of chromatin fiber.

Acknowledgment. We thank Dr. Max Berkowitz and Dr. Michael Rubinstein for insightful comments. This work was supported by the Beckman Young Investigator Award.

JA905376Q